NASA
Technical Memorandum 107201

Army Research Laboratory
Technical Report ARL–TR–1066

A Method to Analyze and Optimize the Load Sharing of Split Path Transmissions

Timothy L. Krantz
Vehicle Propulsion Directorate
U.S. Army Research Laboratory
Lewis Research Center
Cleveland, Ohio

Prepared for the
Seventh International Power Transmission and Gearing Conference
sponsored by the American Society of Mechanical Engineers
San Diego, California, October 6–9, 1996

National Aeronautics and
Space Administration

Trade names or manufacturers' names are used in this report for identification only. This usage does not constitute an official endorsement, either expressed or implied, by the National Aeronautics and Space Administration.

A METHOD TO ANALYZE AND OPTIMIZE THE LOAD SHARING OF SPLIT-PATH TRANSMISSIONS

Timothy L. Krantz
U.S. Army Research Laboratory
Vehicle Propulsion Directorate
Lewis Research Center
Cleveland, Ohio 44135
U.S.A.
(216) 433-3580; Tim.Krantz@lerc.nasa.gov

ABSTRACT

Split-path transmissions are promising alternatives to the common planetary transmissions for rotorcraft. Heretofore, split-path designs proposed for or used in rotorcraft have featured load-sharing devices that add undesirable weight and complexity to the designs. A method was developed to analyze and optimize the load sharing in split-path transmissions without load-sharing devices. The method uses the clocking angle as a design parameter to optimize for equal load sharing. In addition, the clocking angle tolerance necessary to maintain acceptable load sharing can be calculated. The method evaluates the effects of gearshaft twisting and bending, tooth bending, Hertzian deformations within bearings, and movement of bearing supports on load sharing. It was used to study the NASA split-path test gearbox and the U.S. Army's Comanche helicopter main rotor gearbox. Acceptable load sharing was found to be achievable and maintainable by using proven manufacturing processes. The analytical results compare favorably to available experimental data.

INTRODUCTION

The drive system requirements for a rotorcraft are especially demanding. It must transmit the engine power to the rotor while providing a typical speed reduction of 60 to 1. In addition, the drive system must be safe, reliable, lightweight, and energy efficient while producing little vibration and noise. Rotorcraft transmissions have matured to a high performance level through a combination of analyses, experiments, and application of field experiences. Still, the next generation of rotorcraft will call for drive systems that are even safer, lighter, quieter, and more reliable. These improvements are needed to increase vehicle payload and performance, improve passenger comfort and safety, lower operating costs, and reduce unscheduled maintenance.

The weight of the drive system is especially important. It is significantly influenced by three key features of the configuration: the number of stages, the number of parallel power paths, and the gear ratio of the final stage. By using fewer stages, more parallel power paths, and larger reduction ratios at the final stage, the drive system weight can be reduced. More parallel power paths reduce system weight because a gear is sized by mesh loads, not by the total torque. With the total torque shared among multiple meshes, the gear sizes are reduced. Using a larger reduction ratio at the final stage reduces the system weight because the preceding stages then operate at lower torques.

Helicopters typically use a planetary arrangement (Fig. 1) for the final stage of the geartrain. This arrangement usually has 3 to 18 parallel power paths, with a maximum reduction ratio of about 7:1. A little used but promising alternative for the final stage is the split-torque or split-path arrangement (Fig. 2). With the split-path arrangement, a final-stage reduction ratio of up to 14:1 is possible with two parallel power paths. White (1974, 1983, 1984, 1985, 1989) has studied split-path designs and proposed their use in helicopters after concluding that such designs can offer the following advantages over traditional planetary ones:

(1) A high speed reduction ratio at the final stage
(2) A reduced number of gear stages
(3) Lower energy losses
(4) Increased reliability because of separate drive paths
(5) Fewer gears and bearings
(6) Lower noise levels from gear meshes
(7) Lower overall drive system weight

Obviously, depending on the requirements of the vehicle, a split-path design can have significant advantages over the commonly used planetary transmission.

Despite some attractive features, split-path designs have seen little use in rotorcraft, because they have been considered relatively risky. A major risk inherent to these designs is that even gearboxes manufactured to precise tolerances might carry unequal loads in the two parallel paths. To compensate for this, designs proposed for or used in helicopters have featured a load-balancing device. For example, Smirnov (1990) and Cocking (1986) describe split-path designs that feature quill shafts to minimize the torque loading differences between the two parallel load

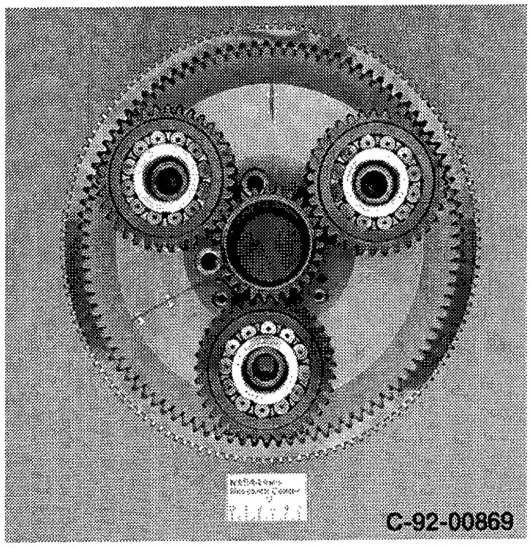

Figure 1.—Planetary design with three load paths used for final stage of helicopter transmission.

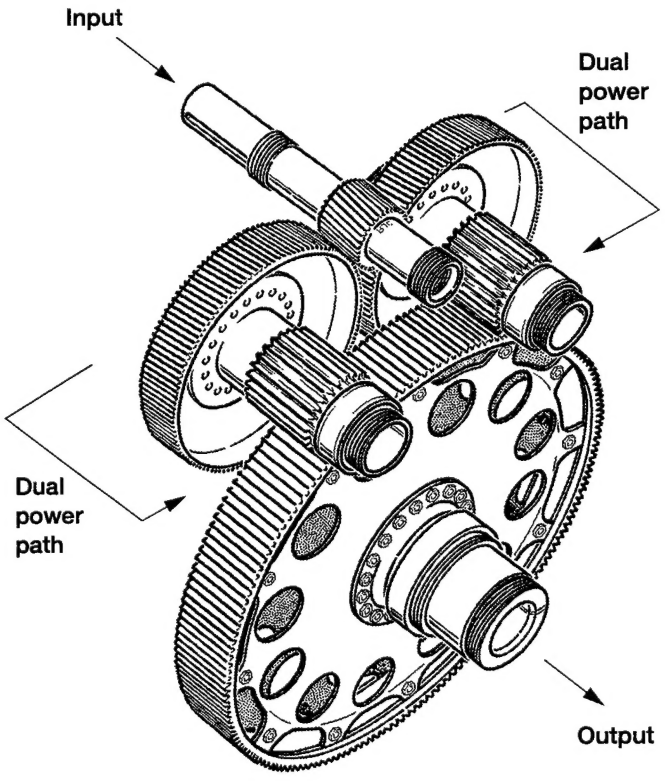

Figure 2.—Example of split-path design with dual power paths.

paths. However, the quill shafts, as do all load-sharing devices, add complexity and weight to the design, thereby offsetting some of the advantages over the proven planetary designs.

Kish (1993a) developed and studied a split-path gearbox that featured a torsionally compliant elastomeric load-sharing device. The gearbox was tested extensively both with and without the load-sharing device, and Kish made the following observations:

(1) Excellent load sharing was obtained when the gearbox was operated under nominal laboratory conditions and with the torsionally compliant load-sharing device installed.

(2) The torsionally compliant load-sharing device that was tested did not meet the requirements for field operation. For example, temperature cycles degraded the function of the device.

(3) Acceptable load sharing can be achieved without a special load-sharing device so long as manufacturing and installation tolerances are adequately controlled. Furthermore, the precision required for manufacture and installation is within the capabilities of available and proven manufacturing processes.

Thus, Kish's research (1993b) indicates that split-path transmissions can be successfully used in rotorcraft and that special load-sharing devices are not necessary. On the basis of this research, a split-path design was selected for use in the U.S. Army's Comanche helicopter. However, the load-sharing properties of such designs are not yet fully understood. For example, Kish (1993a) stated that although acceptable load sharing was demonstrated during the Advanced Rotorcraft Transmission project, the measured load sharing was not as good as had been predicted, considering the precision achieved in the manufacture and installation of the tested gearbox. He suggested that compliances that were not considered in the prediction of the load sharing were, in fact, significant.

The research reported herein was done to help enable the use of split-path transmissions without special load-sharing devices in the Comanche and future rotorcraft. An analytical method was developed and used to study the load-sharing properties of such designs. Here, the clocking angle of the geartrain is defined and shown to be the key design parameter in optimizing an otherwise fixed design for equal sharing of a design load. The load-sharing properties, optimal clocking angle, and effect of manufacturing tolerances are calculated for two gearbox designs—the NASA Lewis split-path test gearbox and the Comanche main rotor gearbox. The analytical predictions are compared to available experimental data. As a companion study, the load sharing of a split-path gearbox was evaluated experimentally. The results of that study are reported separately (Krantz and Delgado, 1996).

SPLIT-PATH CONCEPTS AND DEFINITIONS

In this report, a split path refers to a parallel shaft gearing arrangement, such as that shown in Figs. 2 and 3, where the input pinion meshes with two gears, thereby offering two paths to transfer power to the output gear. Designs that feature a load-sharing device such as an epicyclic torque splitter (White, 1983), balance beam (White, 1989), or quill shaft (Smirnov, 1990; Cocking, 1986) are not considered in this study. This study is limited to split-path designs without a load-sharing device or mechanism.

For purposes of discussion, a coordinate system and some concepts are defined as follows (see Fig. 3): A right-hand Cartesian coordinate system is established such that the z-axis is coincident with the output gear shaft, the positive y-axis extends from the output gear center

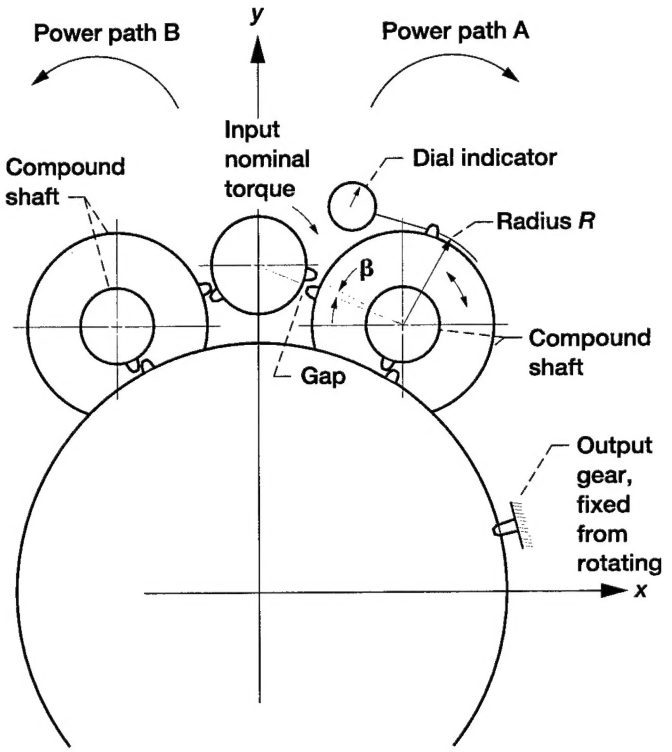

Figure 3.—Illustration of conceptual experiment to measure geartrain clocking angle β.

through the input pinion center, and the input gear drives clockwise. The first-stage gear, gearshaft, and second-stage pinion combination are collectively called the compound shaft. The two power paths are identified as A and B, with A to the right of B.

The clocking of a split-path geartrain is an important attribute. For example, there are certain clockings where the geartrain could not be assembled because some of the gear teeth would interfere with one another. In this report the clocking and load sharing of a split-path geartrain will be shown to be related. Let us describe the clocking by a clocking angle β. Figure 3 shows a method by which this angle could be measured. Here, the output gear is fixed from rotating and a nominal clockwise torque is applied to the input pinion so that the gear teeth come into contact. If all the gear teeth of both power paths come into contact, then the clocking angle β is, by definition, equal to zero. If the teeth of one power path are not in contact, then the clocking angle β is equal to the angle that the first-stage gear would have to be rotated relative to the second-stage pinion to bring all teeth into contact. Clocking angle β could be determined by using a dial indicator to measure the circumferential movement of a gear tooth while rotating the "loose" compound shaft over the range of play and then calculating

$$\beta = X/R \tag{1}$$

where X equals the movement measured by the indicator and R is the radius at which the indicator is located. Under nominal torque, the clocking angle β is defined as positive if a gap exists in path A, and as negative if the gap exists in path B.

To relate the clocking angle to load sharing, we can use the concept of the loaded windup of the geartrain. Envision that the output gear of a geartrain is rigidly fixed from rotating and a torque is applied to the input pinion. As the torque is applied, the input shaft will rotate some amount because of deformations. This rotation of the input pinion relative to the output gear is called the loaded windup. Using the definitions just established, we can see that the loaded windups of the two power paths are related to the clocking angle by

$$\beta = \frac{LWB - LWA}{GR} \tag{2}$$

where LWA = the loaded windup of power path A; LWB = the loaded windup of power path B; and GR = the reduction ratio of the input pinion and compound shaft gear.

The torque transferred by each load path is a product of the loaded windup multiplied by the net torsional stiffness of that path. Considering this fact along with Eq. (2), we can treat the clocking angle β as a design variable. For an otherwise fixed design, the clocking angle can be adjusted to split a design load equally between the two power paths. Of course, as already mentioned, the clocking angle must also allow for assembly of the geartrain.

ANALYTICAL METHOD

An analytical method was developed to study split-path load sharing. In so doing, the following assumptions were made:

(1) The clocking angle β is the only variable dimension; all other dimensions equal the nominal blueprint dimensions.

(2) The significant deformations that contribute to the loaded windups are gearshaft torsion and bending, bearing center movement due to Hertzian deformations at rolling element contacts, gear tooth deflection, and bearing support/housing distortions.

(3) Forces due to friction, thermal expansion, and inertia effects are negligible.

(4) Bearing raceways remain as perfect circles, even under load.

(5) For purposes of calculating gearshaft bending, bearings act as pinned connections and, therefore, do not support reaction moments.

In this method the loaded windups of each load path are calculated for a given input torque and a given load split between the two power paths. The calculated loaded windups can then be used in Eq. (2) to find the clocking angle β. By analyzing an array of input parameters, the relationship between the clocking angle and load sharing can be established for a given input torque. Under the assumptions stated, the gear tooth and bearing reaction force vectors can be calculated by applying gearing kinematics and the methods of statics. Then the deformations within the gearbox, and the windup caused by such deformations, are calculated. In the following paragraphs the calculation of each of the significant deformations is explained.

Gearshaft Torsion

To calculate gearshaft torsion, equivalent torsional spring constants for the shafts were determined. The complex shaft shapes were approximated by using a series of sections having constant cross sections. The torsional spring constants for each section were calculated by

$$K = \frac{L}{JG} \tag{3}$$

where L is the section length, J is the polar moment of inertia, and G is the material's shear modulus. The equivalent torsional spring constants for the shafts were then determined by treating the shafts as a set of torsional springs in series.

Gearshaft Bending

To calculate gearshaft bending, the following classical differential equation for bending was used:

$$EI\frac{d^2y}{dx^2} = M \tag{4}$$

where y is the deflection of the neutral axis, x is a local coordinate along the shaft length, and M (the bending moment), I (the moment of inertia), and E (Young's modulus) each may be a function of coordinate x. To apply the equation, the complex shaft shapes were approximated as a series of sections, each having either a constant or a linearly varying moment of inertia (Fig. 4, for example). Equation (4) was integrated for each of the shaft sections, and the constants of integration were determined by applying matching boundary conditions for the shaft interior and also by assuming zero deflections and moments at the bearing locations. This procedure yielded a set of algebraic equations that were solved simultaneously by matrix algebra. The beam bending for each shaft was calculated twice, once each in two orthogonal planes; the resulting deflections were summed by vector addition.

Bearing Deflections

The force supported by the bearing causes Hertzian deformations at the rolling element contacts and deforms the overall shape of the raceways. In this study, only the Hertzian deformations were considered. The bearing deflections were calculated by an iterative procedure. The first step of the procedure was to guess the radial movement of the bearing center. Then this guess was the input to calculate the total radial deformation of each inner raceway, rolling element, and outer raceway contact. In the third step the radial force that was consistent with the just-calculated radial deformation was calculated for each rolling element contact. This third step was done by trial and error, that is, estimating the radial force on the rolling element and calculating the Hertzian contact deformations with the approximation methods of Hamrock (1991). If these latter deformations equaled those calculated by the second step, then the radial force on the rolling element was considered to have been determined; otherwise, the third step was repeated with a new estimate of the radial force. In the fourth step the radial forces on all the rolling elements were summed, by vector addition, to calculate the bearing support force. Next, the bearing support force calculated in step four was compared with the bearing support force calculated by a static analysis of the gearshaft. If the two calculated forces were approximately equal, then the guess made for the bearing center movement in step one was deemed appropriate, and the bearing deformation was determined. If the forces were not equal, a new guess was made, and the entire process was repeated from step one. Detailed equations are given in the appendix A.

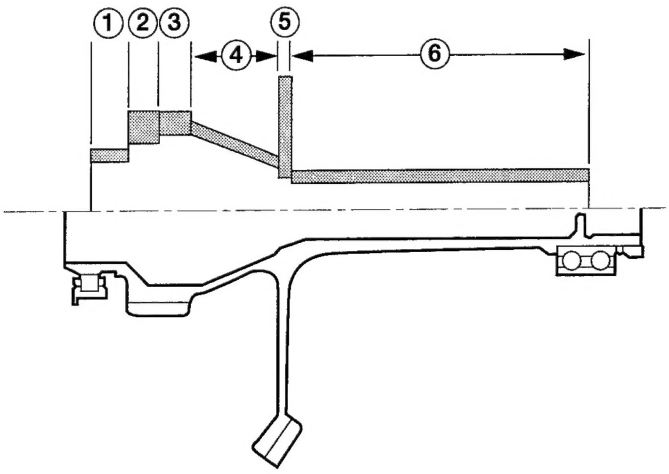

Section number	Moment of inertia	Resistance to bending, kN·m²
1	Constant	50.2
2	Constant	448
3	Constant	364
4	Linear	207 At right end 101 At left end
5	Constant	1662
6	Constant	17.2

Figure 4.—Cross-sectional geometry, approximate geometry, and sectional properties used to predict gearshaft bending.

Gear Tooth Deflections

The gear tooth deflections were calculated by using a spring stiffness equal to the mean of the time-varying mesh stiffness. The mesh stiffness was calculated by using the contact ratio of the gear pair and the method of Cornell (1981) to calculate the stiffness of a pair of contacting spur gear teeth. Cornell's method takes into consideration the effects of the tooth acting as a cantilever beam, the Hertzian contact deformations, the tooth base support, and the contact position. To calculate the mesh stiffness spring constant, the helical gears were modeled as an equivalent set of staggered spur gears. The preprocessor of computer program GEARDYNMULT (Boyd, 1989) was used to do the calculations of Cornell's method.

Bearing Support (Housing) Deflections

For lack of better information or analytical methods, the housing deflections at the bearing support locations were assumed to be in the direction of the bearing net radial force and to be equal in magnitude to one-half of the calculated bearing center movements due to Hertzian deformations.

Once all of the significant deformations were calculated, the resulting loaded windup of each power path was calculated. The loaded windup due to gear teeth deflections, gearshaft torsion, and gear center displacements can be calculated individually and summed by superposition. The loaded windup due to gear teeth deflections and gearshaft torsion was straightforward. The gear center displacements

were calculated as the vector sum of gearshaft bending, bearing center movement, and housing distortion. Then the windup of each load path due to gear center movements was determined by applying the properties of involute gears. Figure 5 illustrates this idea; detailed equations are given in appendix B.

ANALYSIS OF THE NASA LEWIS SPLIT-PATH GEARBOX

The NASA Lewis split-path gearbox was studied by using the newly developed analysis method. This gearbox (Figs. 2 and 6) has two stages and is designed to operate at 373 kW (500 hp) with an input shaft speed of 8780 rpm. Gear and bearing design data are given in Tables I and II. In a case study, the load sharing was optimized at a selected design torque of 406 N-m (3590 in-lb) at the input shaft. The clocking angle tolerance that would produce acceptable load sharing was also calculated. Load sharing was considered acceptable if the more heavily loaded of the split load paths carried no more than 53 percent of the selected design torque. The results are given in Table III. The analysis predicted that the most heavily loaded split path would carry no more than 53 percent of the design torque so long as the clocking angle was maintained within the range –0.00146 to –0.00060 rad (–5.1 to –2.1 min).

To obtain some further insights, the components of the total loaded windup for each load path were calculated for the condition of equal load sharing (Fig. 7). The largest component of the total loaded windup is due to the lateral movements of the second-stage gears. The lateral movements are caused by the combined effects of bearing deformations, housing deformations, and gearshaft bending, and they are very significant because the first-stage gear ratio amplifies their effects. From Eq. (2) we see that since the two power paths have different total loaded windups, the optimal clocking angle deviates from zero. This deviation is entirely due to the lateral movements of the gears; therefore, a torsionally compliant load-sharing device that increases the compliances of both compound shafts by equal amounts would not optimize the load sharing of this gearbox since such a device has no effect on lateral movements.

ANALYSIS OF THE COMANCHE MAIN ROTOR GEARBOX

The Comanche helicopter's main rotor gearbox was analyzed with the newly developed method. This gearbox (Fig. 8) transmits power from two engines to the main and tail rotor shafts. It has three stages: a spiral bevel stage; a spur gear stage, where the load is split; and a double helical stage, where a total of four pinions recombine the power and drive the output gear. The output gear drives the tail rotor shaft through a double helical and bevel mesh. Each engine normally provides power at 820 kW (1100 hp) but can provide 1060 kW (1420 hp) during emergencies (e.g., when one engine is inoperative). Gear and bearing design data are given in Tables IV and V.

The same analytical method that was used to study the NASA Lewis split-path gearbox was used to study the Comanche gearbox, with modifications for calculating the lateral movement of the output gear. For the NASA Lewis gearbox, the movement of the bearing supports was calculated as being in the direction of the net bearing force and equal in magnitude to one-half of the total Hertzian deformations of that bearing. Since results of a finite element analysis of the Comanche gearbox were available (B. Hansen, 1994, Sikorsky Aircraft, personal communication), they were used to model the output gear bearing support stiffness as two springs. (The spring constants used were 16×10^8 N/m (9.0×10^5 lb/in.)

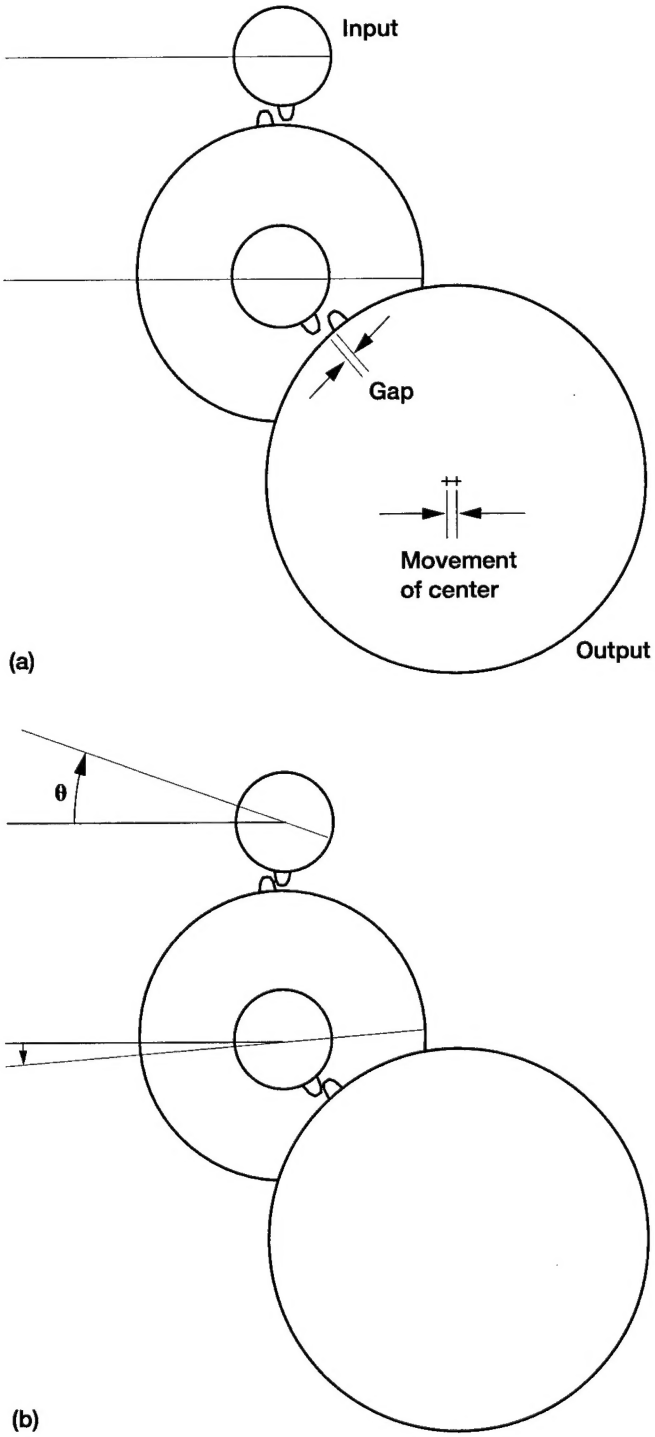

Figure 5.—Illustration showing windup of input pinion θ due to lateral movement of output gear. (a) Gears at initial angular orientations with output gear displaced horizontally. (b) Gears at final angular orientations after rigid body rotations to bring teeth into contact.

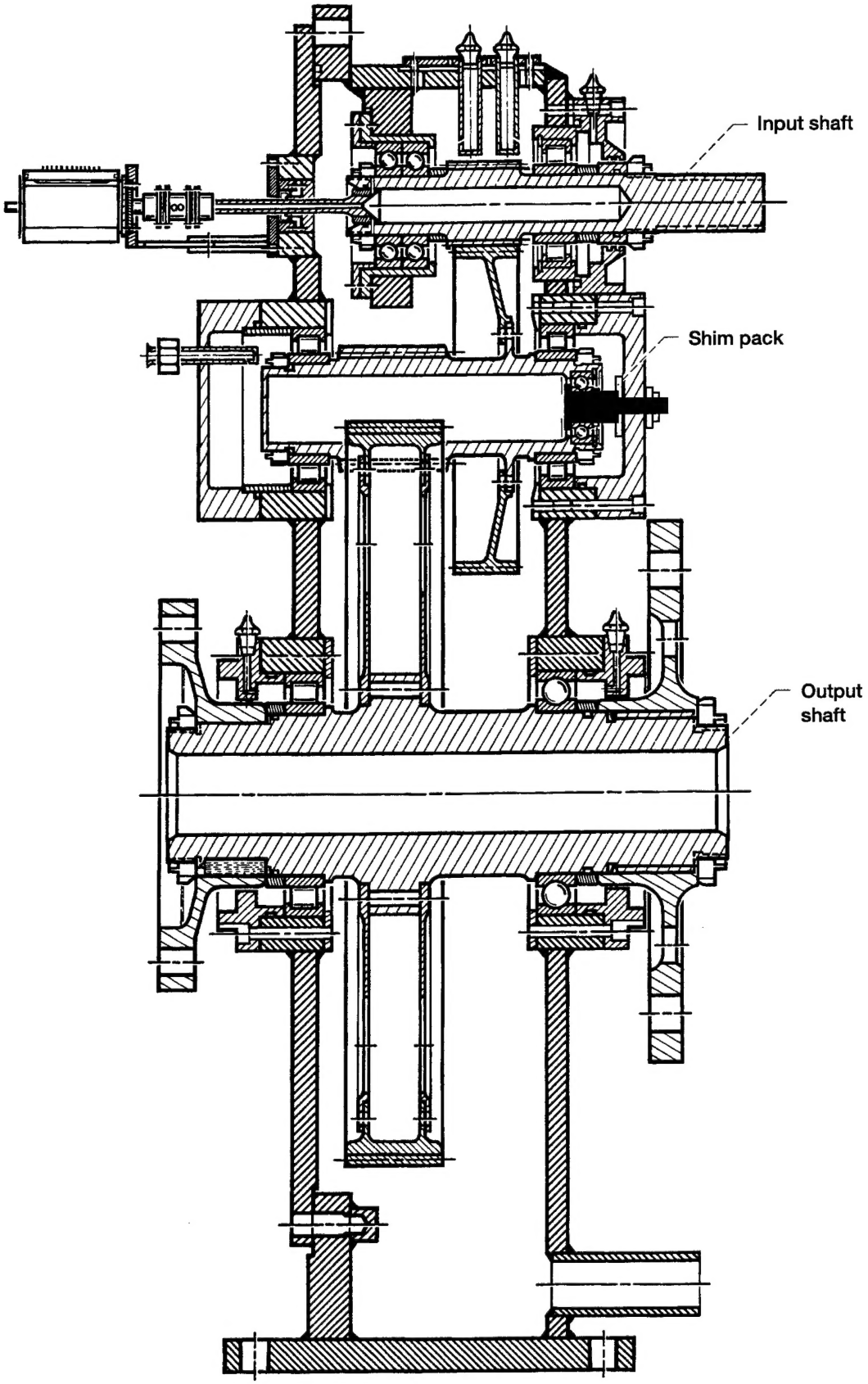

Figure 6.—Cross-sectional view of NASA split-path test gearbox.

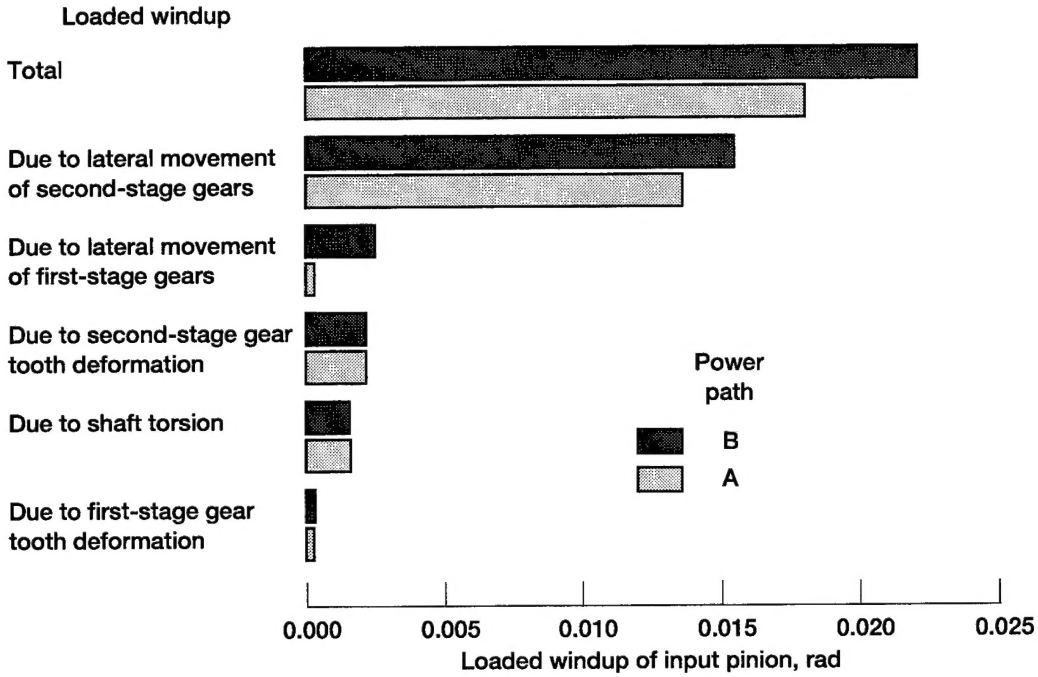

Figure 7.—Total and relative contributions of loaded windups for NASA split-path test gearbox for an input shaft torque of 406 N-m (3590 in.-lb) split equally between the two power paths.

TABLE I.—Gear Data of the NASA Split-Path Test Gearbox

Location	Number of teeth	Pitch diameter, mm	Face width, mm	Normal pressure angle, deg	Helix angle, deg
First-stage pinion	32	51.1	44.5	20	6
First-stage gear	124	197.9	38.1	20	6
Second-stage pinion	27	68.6	66.0	25	0
Second-stage gear	176	447.0	59.9	25	0

TABLE II.—Bearing Data of the NASA Split-Path Test Gearbox

Location	Type	Inner raceway diameter, mm	Outer raceway diameter, mm	Number of rolling elements	Rolling element diameter, mm	Roller length, mm	Contact angle, deg
Input shaft	Roller	50.0	69.1	13	9.53	13.20	-
Compound shaft	Roller	87.4	66.5	15	10.67	10.67	-
Output shaft	Roller	113.0	133.9	23	15.88	10.41	-
Input shaft	Duplex ball	48.9	71.3	14	11.13	—	29
Output shaft	Ball	109.1	140.9	14	15.88	—	0

TABLE III.—Predicted Relationship Between Load Sharing and Clocking Angle for NASA Split-Path Test Gearbox

[Input shaft torque, 405.6 N-m.]

Load, percent		Loaded windup, rad		Clocking angle, rad
Path A	Path B	Path A	Path B	
47	53	0.01728	0.02293	-0.00146
50	50	.01801	.02199	-.00103
53	47	.01874	.02105	-.00060

TABLE IV.—Gear Data of the Comanche Main Rotor Gearbox

Location	Number of teeth	Pitch diameter, mm	Face width, mm	Normal pressure angle, deg	Helix or spiral angle, deg
First stage					
Bevel pinion[a]	31	115.7	23.0	20	32
Bevel gear[a]	63	235.1	23.0	20	32
Second stage					
Spur pinion	33	92.0	25.7	22.5	0
Spur gear	95	265.0	25.7	22.5	0
Third stage					
Double helical pinion	13	58.4	[b]31.6	20	35
Double helical gear	144	647.2	[b]34.4	20	35

[a]Bevel mesh has shaft angle of 77°.
[b]Each half of the double helical members.

TABLE V.—Bearing Data of the Comanche Main Rotor Gearbox

Location	Type	Pitch diameter, mm	Rolling elements per row	Rolling element diameter, mm	Roller length, mm	Contact angle, deg
First-stage bevel pinion						
Outboard	Spherical roller	67.8	16	11.0	15.0	13.4
Inboard	Roller	65.4	18	9.0	9.0	0
First/second-stage shaft						
Upper	Roller	77.5	18	11.0	11.0	0
Lower	Duplex ball	54.0	19	7.9	—	20.0
Second/third-stage shaft						
Upper	Roller	77.5	14	14.0	14.0	0
Lower	Roller	80.0	10	19.0	19.0	0
Third-stage output shaft	Tapered roller	381.8	100	8.8	13.2	16.5

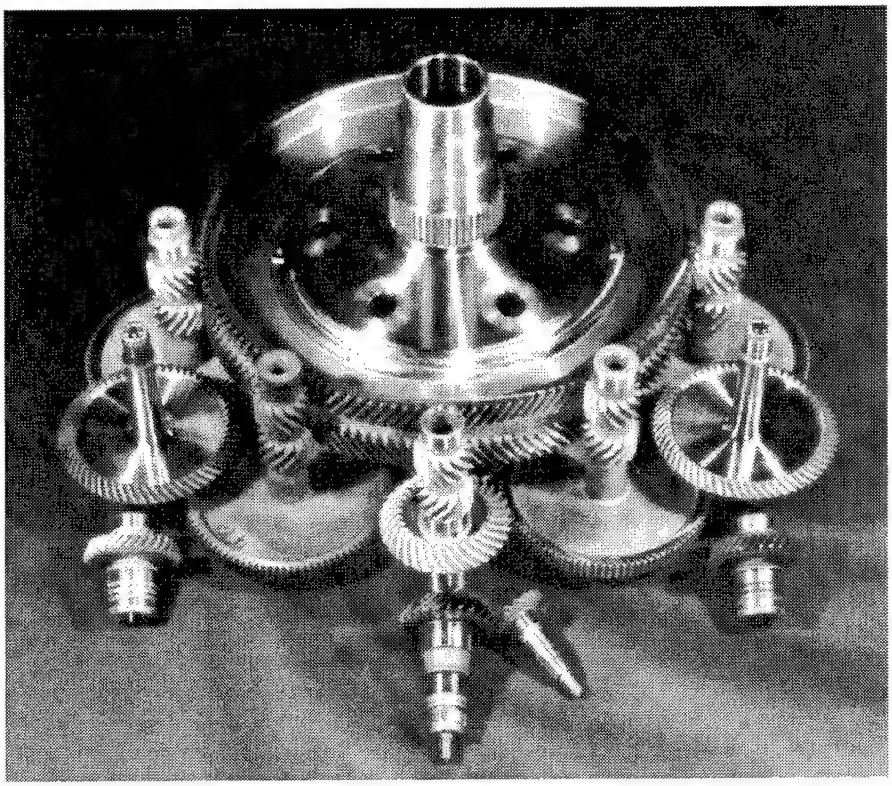

Figure 8.—Split-path design for two engines used for Comanche helicopter.

along the aircraft centerline and 6.0×10^8 N/m (3.5×10^5 lb/in.) perpendicular to the centerline.) The output gear of the Comanche gearbox is supported by a tapered roller bearing, but the developed analytical method is valid only for straight roller bearings. With the assumption that the deflection of the tapered roller bearing would be equal to that of an "equivalent" straight roller bearing, an equivalent bearing was defined. The cross section geometry of the tapered roller bearing midway along the roller length was used to define the geometry of the equivalent straight bearing for purposes of calculating the bearing deflection.

The optimal clocking angle for each engine load path that would produce equal loads in each split path with both engines operating at normal flight power was calculated. Also, each path's allowable clocking angle tolerance was determined such that the most heavily loaded split path would carry no more than 53 percent of the power of one engine. The results, presented in Table VI, show that so long as the clocking angles are maintained to within –0.00070 to +0.00176 rad (–2.4 to +6.1 min) for engine 1 and to within +0.00331 to +0.00584 rad (+10.7 to +20.1 min) for engine 2 the 53-percent-load maximum can be achieved.

TABLE VI.—Predicted Relationship Between Load Sharing and Clocking Angle for the Comanche Main Rotor Gearbox

[Engines operating at 820 kW (1100 hp) per engine.]

Power in each load path, percent				Engine 1			Engine 2		
Engine 1		Engine 2		Loaded windup, rad		Clocking angle, rad	Loaded windup, rad		Clocking angle, rad
Path A	Path B	Path A	Path B	Path A	Path B		Path A	Path B	
50	50	50	50	0.0321	0.0336	+0.00053	0.0261	0.0393	+0.00458
53	47	53	47	.0335	.0315	-.00070	.0279	.0374	+.00331
53	47	47	53	.0343	.0318	-.00086	.0244	.0416	+.00600
47	53	53	47	.0299	.0355	+.00192	.0278	.0369	+.00315
47	53	47	53	.0307	.0358	+.00176	.0243	.0411	+.00584

TABLE VII.—Predicted Load Sharing for the Comanche Main Rotor Gearbox Operating Under Emergency[a] Conditions for Clocking Angles That Maintain a 53- to 47-Percent Load Split Under Cruise Conditions

[Cruise power = 820 kW (1100 hp) per engine; emergency condition power = 1059 kW (1420 hp).]

Clocking angles in assembled configuration, rad		Engine 1 power to path A, percent		Engine 2 power to path B, percent	
Engine 1	Engine 2	At cruise condition	With one engine inoperative	At cruise condition	With one engine inoperative
At nominal clocking angles					
+0.00053	+0.00458	50.0	53.5	50.0	54.2
At maximum clocking angles					
+0.00176	+0.00584	47.0	51.2	53.0	56.4
At minimum clocking angles					
-0.00070	+0.00331	53.0	55.7	47.0	52.0

[a]Emergency condition is defined as one engine inoperative.

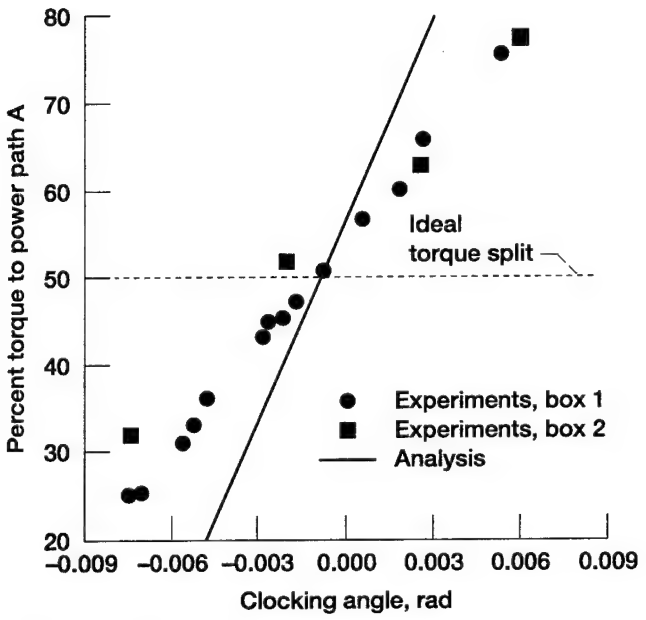

Figure 9.—Experimental data and analytical predictions of percentage of total torque to power path A as a function of clocking angle for NASA split-path test gearbox; input shaft torque of 367 N-m (3250 in.-lb).

It is reasonable to expect that these tolerances can be maintained during manufacture. Therefore, split-path transmissions without load-sharing devices can be built so as to maintain acceptable load sharing by using proven manufacturing capabilities. This is encouraging evidence that these transmissions could be successfully used for rotorcraft.

TABLE VIII.—Experimentally and Analytically Determined Power Distribution Among Split Paths of Comanche Main Rotor Gearbox

[Input shaft power = 820 kW (1100 hp) per engine.]

Ranking by load level	Engine number	Power path	Engine power transmitted by split path, percent	
			Experiment	Analysis
1	2	A	58	60
2	1	A	53	52
3	1	B	47	48
4	2	B	42	40

The load sharing of the Comanche gearbox operating under emergency conditions (with one inoperative engine) was studied. The clocking angles considered in this part of the study were those that provided acceptable load sharing under normal operating flight power. Results of the calculations are presented in Table VII. Under normal flight power and with the clocking angles at maximum acceptable dimensions, the most heavily loaded split path will carry 435 kW (583 hp) or 53.0 percent of an engine's normal flight power. For the same clocking angles and with only engine 2 operating, the most heavily loaded split path will carry 597 kW (801 hp) or 56.4 percent of emergency condition power. During the emergency power condition, the power output of the operating engine increases by 29 percent over the normal flight condition, but the power carried by the most heavily loaded split path may increase by as much as 37 percent. Thus the load sharing of a split-path gearbox under normal two-engine conditions can be very different from the load sharing for emergency, one-engine-inoperative power conditions.

COMPARISON OF ANALYTICAL AND EXPERIMENTAL RESULTS

The results of this analytical study were compared to the results of the companion experimental study (Krantz and Delgado, 1996). Results describing the percentage of the total torque carried by power path A as a function of the clocking angle are compared in Fig. 9. Both the analyses and experiments indicate that power path A will carry the desired 50 percent of the total torque at a clocking angle of approximately –0.001 rad. For a given clocking angle deviation from the optimal value, the analysis predicts a somewhat greater deviation from equal load sharing than was measured experimentally. For example, if 53 to 47 percent of the total torque is considered the acceptable load for power path A, the analysis suggests a tolerance for the clocking angle of about ± 0.0004 rad, whereas the experiments suggest the tolerance was about ± 0.0007 rad.

Analyses were also conducted to predict the results of experiments done to measure the load sharing of the prototype main rotor gearbox for the Comanche helicopter. The prototype gearbox was designed for nominal clocking angles of zero for both engines. The results of the experiment indicate that the clocking angles of the tested gearbox were indeed near zero (experimental work done by J. Kish, 1995, Sikorsky Aircraft; personal communication). Experimental and analytical results are compared in Table VIII. The analytically predicted rankings of the split paths (from highest to lowest loads) are confirmed by the experiments. The measured and predicted loads for the individual split paths match to within about 3 percent of one engine's power. For both gearboxes studied, the analytical predictions compare favorably to the experimental results.

The differences between the analytical and experimental results presented here are probably due to the net effects of several assumptions made in developing the analytical method. One significant assumption was that the bearing races remained as perfect circles, even under load. A second significant assumption was that the magnitude of the housing deformations at the bearing supports equaled one-half of the bearing center movements due to rolling element and raceway deformations. If a more precise analysis is desired, perhaps the validity of these two assumptions should be assessed

SUMMARY

This investigation was done to better understand split-path transmissions without load-sharing devices and to support their use in the Comanche and in future rotorcraft. An analytical method was developed to calculate the effects of deformations on load sharing. This method was applied to both the NASA split-path gearbox and the Comanche main rotor gearbox. The following results and conclusions were obtained:

1. The clocking angle can be considered a design variable for split-path gearboxes. For an otherwise fixed design, the clocking angle can be adjusted to split a design load equally between the two power paths.

2. For the NASA split-path gearbox, the analysis predicts that the most heavily loaded split path will carry no more than 53 percent of the design torque so long as the clocking angle is maintained within the range –0.00146 to –0.00060 rad (–5.0 to –2.1 min).

3. For the Comanche main rotor gearbox, the most heavily loaded split path will carry no greater than 53 percent of one engine power so long as the clocking angles are kept to within –0.00070 to +0.00176 rad (–2.4 to 6.1 min) for engine 1 and to within +0.00331 to +0.00584 rad (+11.4 to +20.1 min) for engine 2.

4. The load sharing of a split-path gearbox with two engines operating under normal flight conditions can be very different from the load sharing for emergency (one-engine-inoperative) power conditions.

5. The analytical predictions compare favorably to experimental data.

6. Split-path transmissions without load-sharing devices can be built to maintain acceptable load sharing by using proven manufacturing capabilities. This is encouraging evidence that these transmissions could be successfully used for rotorcraft.

ACKNOWLEDGMENT

The author thanks Gene Kish, Charlie Isabelle, Bruce Hansen, Robert Durwin, and Gregg Ambrose of Sikorsky Aircraft for providing Comanche data and for their interest, guidance, and support.

REFERENCES

Boyd, L.S.; and Pike, J.A., 1987, "Expansion of Epicyclic Gear Dynamic Analysis Program," NASA CR–179563, NASA Lewis Research Center, Cleveland, OH.

Cocking, H., 1986, "The Design of an Advanced Engineering Gearbox, *Vertica*, Vol. 10, No. 2, Westland Helicopters and Hovercraft PLC, Yeovil, England, pp. 213–215.

Cornell, R.W., 1981, "Compliance and Stress Sensitivity of Spur Gear Teeth," *J. Mech. Des. Trans.*, ASME, Vol. 103, pp 447–459.

Hamrock, B.J., 1991, "Fundamentals of Fluid Film Lubrication," NASA RP–1255, NASA Lewis Research Center, Cleveland, OH.

Kish, J.G., 1993a, "Sikorsky Aircraft Advanced Rotorcraft Transmission (ART) Program-Final Report," NASA CR-191079, NASA Lewis Research Center, Cleveland, OH.

Kish, J., 1993b, "Comanche Drive System," *Rotary Wing Propulsion Specialists' Meeting: Proceedings, American Helicopter Society*, Williamsburg, VA, p. 7.

Krantz, T.; and Delgado, I., 1996, "Experimental Study of Split-Path Transmission Load Sharing," NASA TM–107202, ARL TR–1067, NASA Lewis Research Center, Cleveland, OH.

Smirnov, G., 1990, "Multiple-Power-Path Nonplanetary Main Gearbox of the Mi-26 Heavy-Lift Transport Helicopter," *Vertiflite*, Mil Design Bureau, Moscow, Vol. 36, pp. 20–23.

White, G.. 1974, "New Family of High-Ratio Reduction Gear With Multiple Drive Paths," *Proc. Instn. Mech. Engrs.*, Vol. 188, pp. 281–288.

White, G., 1983, "Design Study of a 375-kW Helicopter Transmission With Split-Torque Epicyclic and Bevel Drive Stages," *J. Mech. Eng. Sci.*, Vol. 197, Part C, pp. 213–224.

White, G., 1984, "A 2400-kW Lightweight Helicopter Transmission With Split-Torque Gear Trains," ASME Paper 84-Det-91.

White, G., 1985, "The 3600 hp Split-Torque Helicopter Transmission," NASA CR–174932, NASA Lewis Research Center, Cleveland, OH.

White, G., 1989, "Split-Torque Helicopter Transmission With Widely Separated Engines," *Proc. Instn. Mech. Engrs.*, Vol. 203, No. G1, pp. 53–65.

APPENDIX A
CALCULATION OF THE DEFORMATIONS OF ROLLING ELEMENT AND RACEWAY CONTACTS

The methods presented by Hamrock (1991) were used to calculate the deformations of rolling element and raceway contacts. The equations that follow are approximate solutions of the classical Hertzian theories. Material properties are introduced into the calculations by defining an effective elastic modulus E' as

$$E' = \frac{2}{\frac{1-\nu_1^2}{E_1} + \frac{1-\nu_2^2}{E_2}} \tag{A1}$$

where E = Young's modulus, ν = Poisson's ratio, and the subscripts 1 and 2 indicate the rolling element and raceway materials, respectively. For cylindrical roller bearings, the curvatures of the bearing geometry are introduced into the calculation by

$$R_x = \frac{r_{bx} r_{ax}}{r_{bx} \pm r_{ax}} \tag{A2}$$

where r_{bx} is the raceway radius, r_{ax} is the roller radius, the plus sign designates an inner raceway, and the minus sign designates an outer raceway. The dimensionless load W' is defined as

$$W' = \frac{F}{E' R_x l} \tag{A3}$$

where F is the load on a single rolling element and l is the rolling element's effective length. The contact semiwidth b is calculated by

$$b = R_x \left\{ \frac{8W'}{\pi} \right\}^{1/2} \tag{A4}$$

The maximum deformation of a roller raceway contact Δ_{roll} is then calculated by

$$\Delta_{roll} = \frac{2W'R_x}{\pi} \left\{ \frac{2}{3} + \ln\left(\frac{2r_{ax}}{b} \right) + \ln\left(\frac{2r_{bx}}{b} \right) \right\} \tag{A5}$$

For ball bearings, the conformity of the geometry is introduced into the calculations by

$$f = \frac{r}{d} \tag{A6}$$

where r is the raceway groove radius and d is the ball diameter (Fig. 10). The curvatures of the ball bearing geometries are calculated by

$$R_y = \frac{fd}{2f - 1} \tag{A7}$$

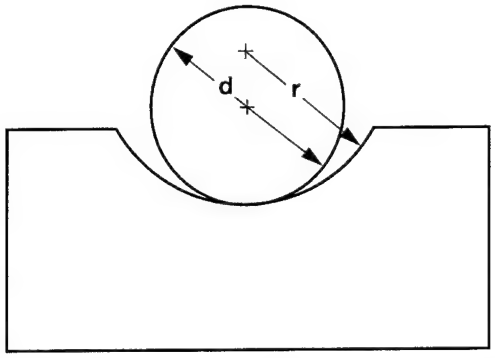

Figure 10.—Cross-sectional geometry of ball and outer race showing race conformity.

$$R_x = \frac{d\left\{ \frac{1}{2}\left(d_o + d_i\right) \pm d\cos(\gamma) \right\}}{d_o + d_i} \tag{A8}$$

where d_o is the outer raceway diameter (the inner diameter of the out race), d_i is the inner raceway diameter, d is the ball diameter, γ is the bearing contact angle, the plus sign designates an outer raceway contact, and the minus sign designates an inner raceway contact. The curvature sum R is defined as

$$R = \left\{ \frac{1}{R_x} + \frac{1}{R_y} \right\}^{-1} \tag{A9}$$

The curvature ratio α is defined as

$$\alpha = \frac{R_y}{R_x} \tag{A10}$$

The Hertzian contact ellipticity parameter K is then calculated as

$$K = \alpha^{\{2/\pi\}} \tag{A11}$$

and the elliptical integral terms C and A as

$$C = 1 + \frac{\left\{ \frac{\pi}{2} - 1 \right\}}{\alpha} \tag{A12}$$

$$A = \frac{\pi}{2} + \left\{ \frac{\pi}{2} - 1 \right\} \ln \alpha \tag{A13}$$

The maximum deformation in a ball and raceway contact Δ_{ball} can then be calculated as

$$\Delta_{ball} = A\left\{\left(\frac{9}{2CR}\right)\left(\frac{F}{\pi KE'}\right)^2\right\}^{1/3} \qquad \text{(A14)}$$

where F is the load carried by a single ball. These methods were used to calculate the load carried by each rolling element of the bearing, and all of the load vectors were summed to calculate a net bearing load. The relation between the net radial load and radial deformation for a rolling element bearing is typically nonlinear, as illustrated by Fig. 11. The following FORTRAN subroutines were used to do the calculations for this study:

FORTRAN subroutine for roller bearing deflections:

```
      subroutine rolldf
     (tl,dr,di,do,rl,er,prr,ei,pri,eo,pro,a,ai,ao)
c
c     subroutine to calculate the deflection for a single
c     roller element, inner race, outer race conjunction for
c     roller bearings
c
c     version 1.0  6/22/93  tim krantz
c     version 1.1  12/27/93 changed name to 6 letters to keep
c     within standard FORTRAN convention
c     version 1.2  2/7/94   changed coefficients within log
c     expressions from 4 to 2, per NASA RP-1126
c
c
c     Hertzian calculations are based on equations in
c     NASA RP-1126, Lubrication of Machine Elements
c     (Hamrock, 1991).
c
c     required inputs
c
c       tl  = total load
c       dr  = roller diameter
c       di  = inner raceway diameter
c       do  = outer raceway diameter
c       rl  = roller length
c       er  = Young's modulus for roller
c       prr = Poisson's ratio for roller
c       ei  = Young's modulus for inner race
c       pri = Poisson's ratio for inner race
c       eo  = Young's modulus for outer race
c       pro = Poisson's ratio for outer race
c
c     outputs
c
c       a   = total deformation
c       ai  = inner race deformation
c       ao  = outer race deformation
c
c=====================================================
c
c     calculate elastic coefficients
c
c       inner race & roller
c
        eroll=(1.-prr*prr)/er
        eirac=(1.-pri*pri)/ei
        epi=2./(eroll+eirac)
c
c       outer race & roller
c
        eorac=(1.-pro*pro)/eo
        epo=2./(eroll+eorac)
```

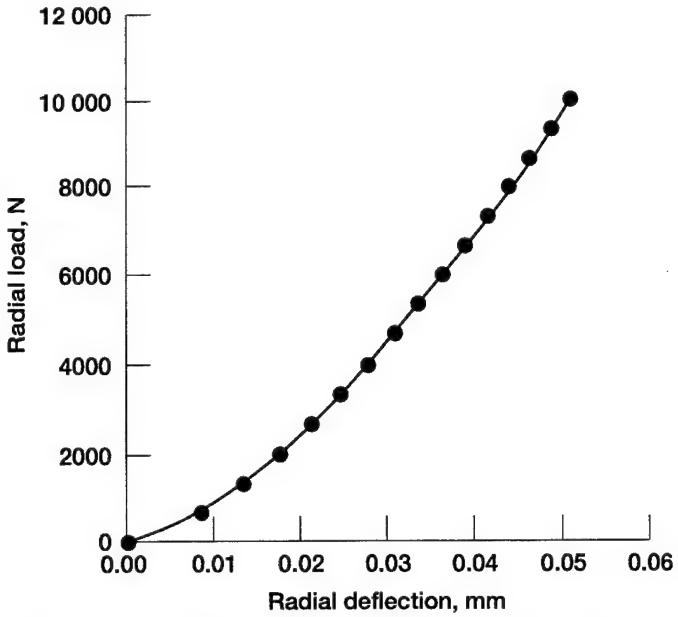

Figure 11.—Example of typical nonlinear function relating radial deflection of rolling element bearing to radial load.

```
c
c     calculate curvature terms
c
        rax=dr/2.
        rbxi=di/2.
        rbxo=do/2.
        rxi=(rax*rbxi)/(rbxi+rax)
        rxo=(rax*rbxo)/(rbxo-rax)
c
c     calculate outer race & roller deformation
c
       uload=tl/rl
       wprime=uload/(epo*rxo)
       b=rxo*sqrt(8.*wprime/3.141592)
       coeff=2.*wprime*rxo/3.141492
       ao=coeff*(2./3.+log(2.*rax/b)+log(2.*rbxo/b))
c
c     calculate inner race & roller deformation
c
       wprime=uload/(epi*rxi)
       b=rxi*sqrt(8.*wprime/3.141592)
       coeff=2.*wprime*rxi/3.141492
       ai=coeff*(2./3.+log(2.*rax/b)+log(2.*rbxi/b))
c
c     total deformation is sum of inner and outer
c     race conjunctions
c
        a=ai+ao
        return
        end
```

FORTRAN subroutine for ball bearing deflections:

```
      subroutine balldf(tl,d,di,do,fi,fo,del)
c
c     subroutine to calculate the deflection for a single
c     rolling element, pure radially loaded inner
c     race-ball-outer race conjunction-to be used for
c     calculating ball bearing deflections
```

```
c
c   version 1.0  1/31/94  tim krantz
c   version 1.1  2/3/94   correct typo for calculation
c   of ki and ko
c
c   Hertzian calculations are based on equations in
c   NASA RP-1126, Lubrication of Machine Elements
c   (Hamrock, 1991, p. 78)
c
c   required inputs
c
c     tl     = total load (lb)
c      d     = ball diameter (in.)
c     di     = inner raceway diameter (in.)
c     do     = outer raceway diameter (in.)
c     fi     = inner race conformity ** see notes
c     fo     = outer race conformity ** see notes
c
c   outputs
c
c   del      = total deformation in direction of
c              applied load
c
c=======================================================
c
c  Notes:
c
c   1.  It is assumed that the material is steel
c        with E=30e+06 and Poisson's ratio = 0.29.
c
c   2.  The race conformities (f) are often not
c       available in bearing catalogs. By definition,
c       the race conformity is greater than or equal
c       to 0.5. Most bearings are in the range
c       0.51<f<0.54, with f = 0.52 the most common
c       value. Often, the outer race conformity is
c       smaller than the inner race conformity in order
c       to equalize the contact stresses of the inner
c       and outer races. The difference in conformities
c       usually does not exceed 0.02.
c
c=======================================================
c
c
c
      real ki,ko
      pi=atan(1.)*4.
      eprim=32.755e+06
c
c   calculate curvature terms
c
      de=0.5*(do+di)
      rxi=d*(de-d)/(2.*de)
      rxo=d*(de+d)/(2.*de)
      ryi=fi*d/(2.*fi-1.)
      ryo=fo*d/(2.*fo-1.)
      ri=1./(1./rxi+1./ryi)
      ro=1./(1./rxo+1./ryo)
      alphi=ryi/rxi
      alpho=ryo/rxo
      ki=alphi**(2./pi)
      ko=alpho**(2./pi)
      q=(pi/2.)-1.
      ei=1+(q/alphi)
      eo=1+(q/alpho)
      ffi=(pi/2.)+q*log(alphi)
      ffo=(pi/2.)+q*log(alpho)
      t1=9./(2.*ei*ri)
      t2=tl/(pi*ki*eprim)
      deli=ffi*((t1*t2*t2)**(1./3.))
      t1=9./(2.*eo*ro)
      t2=tl/(pi*ko*eprim)
      delo=ffo*((t1*t2*t2)**(1./3.))
c
      del=deli+delo
      return
      end
```

Appendix B
Calculation of Pinion Windup Resulting From the Movements of Gear Centers

The properties of the involute were used to calculate the pinion windup resulting from the movements of the gear centers. These movements occur because of gear support forces that arise when torque is carried by the gear pair. In the description that follows, a gear's angular orientation is defined as the polar angle, in the global coordinate system, of the vector originating at the gear center and ending at the intersection of the gear's base circle and the involute curve of interest. If we use the gear member as a reference, the pinion windup is the difference between the pinion's angular orientations when the geartrain is loaded and that when the geartrain is unloaded.

To calculate the angular orientation of the gear under no load, we use the known radii of the base circles, the global X-Y Cartesian coordinates of the gear centers, and the radial distance from the gear center to the contact point along the line-of-action (Fig. 12). We also establish a local X'-Y' coordinate system such that the Y' axis is coincident with the line-of-centers. Further, we assume that the driving member rotates clockwise (see Eqs. (B16) to (B18) in this appendix for the case of the driving member rotating counterclockwise). The angle Ω_1 that relates the global and local coordinate systems is given by

$$\Omega_1 = arctangent\left\{\frac{Y_{P1}-Y_{G1}}{X_{P1}-X_{G1}}\right\}-\frac{\pi}{2} \qquad \text{(B1)}$$

The installed center distance and pressure angles are

$$\overline{MN} = \sqrt{\{X_{P1}-X_{G1}\}^2+\{Y_{P1}-Y_{G1}\}^2} \qquad \text{(B2)}$$

$$\eta_1 = arccosine\left\{\frac{r_p+r_g}{\overline{MN}}\right\} \qquad \text{(B3)}$$

Next, the length of line segment AB may be calculated from the properties of right triangle ABM, since the length of line segment BM is known to be equal to the radius to the contact point:

$$\overline{AB} = \sqrt{\left\{\overline{BM}\right\}^2 - r_g^2} \qquad \text{(B4)}$$

By the properties of the involute, the length of line segment AB equals arc length AC. Therefore, angle λ_1 may be calculated as

$$\lambda_1 = \frac{\overline{AB}}{r_g} \qquad \text{(B5)}$$

In Fig. 12, we see that Ω_1 is positive counterclockwise, so the gear angular orientation angle σ_g can be calculated by

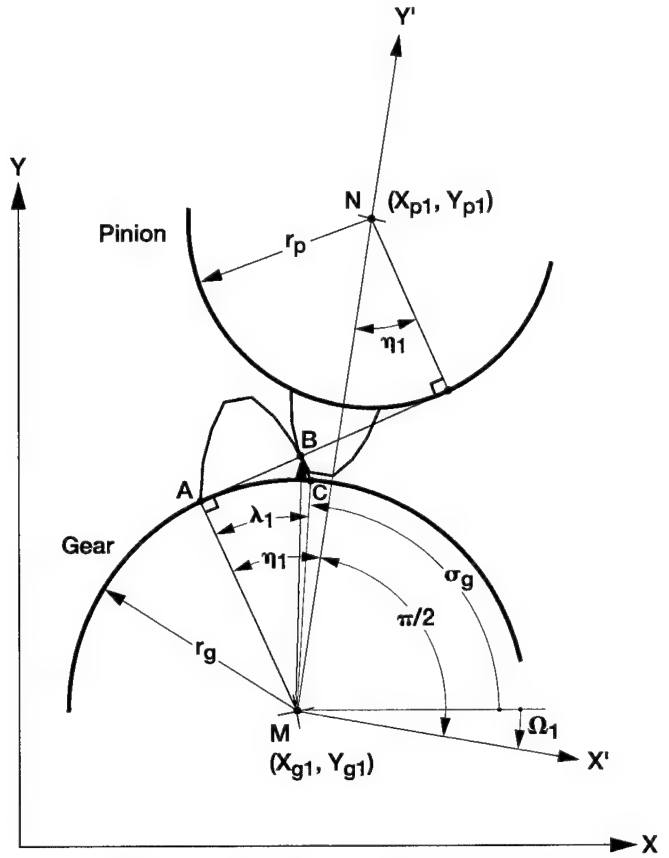

Figure 12.—Coordinate systems and variables to calculate pinion orientation angle with radius contact point.

$$\sigma_g = \frac{\pi}{2}+\eta_1-\lambda_1+\Omega_1 \qquad \text{(B6)}$$

Equations (B1) to (B6) establish a general procedure for calculating the gear angular orientation angle.

Equations (B7) to (B15) establish a general procedure to calculate the pinion angular orientation angle if the gear centers' coordinates, the radii of the base circles, and the gear angular orientation angle σ_g (Fig. 13) are known. A local X''-Y'' coordinate system is established such that the Y''-axis is coincident with the line-of-centers. The angle Ω_2 that relates the local and global coordinate systems is given as

$$\Omega_2 = arctangent\left\{\frac{Y_{P2}-Y_{G2}}{X_{P2}-X_{G2}}\right\}-\frac{\pi}{2} \qquad \text{(B7)}$$

The operating center distance and pressure angles can be calculated as

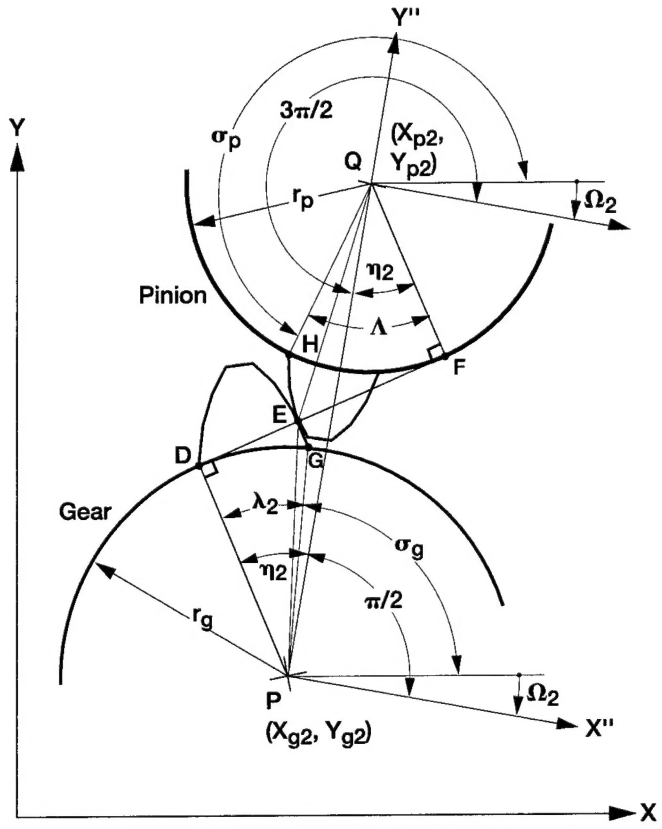

Figure 13.—Coordinate systems and variables to calculate pinion orientation angle from gear angular orientation angle.

$$\overline{PQ} = \sqrt{\{X_{P2} - X_{G2}\}^2 + \{Y_{P2} - Y_{G2}\}^2} \tag{B8}$$

$$\eta_2 = arccosine\left\{\frac{r_p + r_g}{\overline{PQ}}\right\} \tag{B9}$$

Since the gear angular orientation is known, angle λ_2 can be calculated by

$$\lambda_2 = \frac{\pi}{2} + \eta_2 + \Omega_2 - \sigma_g \tag{B10}$$

By the properties of the involute, arc length DG equals the length of line segment DE, and therefore,

$$\overline{DE} = \lambda_2 r_g \tag{B11}$$

The length of line segment DF can be determined from the properties of right triangles as

$$\overline{DF} = \{r_g + r_p\}\text{tangent}\{\eta_2\} \tag{B12}$$

The length of line segment EF can be found by subtraction

$$\overline{EF} = \overline{DF} - \overline{DE} \tag{B13}$$

By the properties of the involute, arc length FH equals the length of line segment EF, so angle Λ can be calculated from

$$\Lambda = \frac{\overline{EF}}{r_p} \tag{B14}$$

Finally, the pinion angular orientation angle σ_p can be calculated from

$$\sigma_p = \frac{3\pi}{2} + \eta_2 - \Lambda + \Omega_2 \tag{B15}$$

To apply the just-described procedure to calculate loaded windup, we assume that the geartrain is unloaded and (without loss of generality) that the gear pair is operating at the pitch point. Then Eqs. (B1) to (B6) may be used to calculate the gear angular orientation angle. Equations (B7) to (B15) may then immediately be applied to calculate the pinion's angular orientation angle under zero load. Next, we use new values for the gear centers' locations (the deformed locations after load is applied) and, keeping the same value for the gear angular orientation angle, again apply Eqs. (B7) to (B15) to calculate the pinion angular orientation angle with load applied. Subtracting the pinion angular orientation angles (the loaded angle minus the zero load angle) yields the pinion loaded windup.

The procedure just developed is valid for the driving member rotating clockwise. For the case of the driving member rotating counterclockwise, the same procedure may be used if the following three changes are made:

Substitute the following equation for Eq. (B6):

$$\sigma_g = \frac{\pi}{2} - \eta_1 + \lambda_1 + \Omega_1 \tag{B16}$$

Substitute the following equation for Eq. (B10):

$$\lambda_2 = \sigma_g - \Omega_2 - \left\{\frac{\pi}{2} - \eta_2\right\} \tag{B17}$$

Substitute the following equation for Eq. (B15):

$$\sigma_p = \frac{3\pi}{2} - \eta_2 + \Lambda + \Omega_2 \tag{B18}$$

In this study, the following FORTRAN subroutines, which are valid for the case of the driving member rotating clockwise, were used to calculate pinion loaded windup due to movements of the gear centers. A companion routine called ANGLE is also listed.

FORTRAN subroutines used for loaded windup calculations

```
      subroutine gearao(xp,yp,rp,xg,yg,rg,rcpg,thetag)
c
c     gearao - FORTRAN subroutine to calculate the
c     GEAR Angular Orientation (GEARAO)in the global
c     coordinate system. The angular orientation is
c     defined by the angle from the global X-axis to
c     the vector originating at the gear center and
c     ending at the intersection of the base circle
c     and the involute curve. The returned angle is
c     positive for counterclockwise.
c
c     written by Tim Krantz
c
c     Version  1.0    11/29/93
c
c-----------------------------------------
c
c     list of arguments
c
c     inputs
c
c       xp,yp    = global coordinates of pinion center
c       xg,yg    = global coordinates of gear center
c
c       rp       = base radius of pinion
c       rg       = base radius of gear
c
c       rcpg     = radius to contact point on gear
c
c     outputs
c
c       thetag   = angular location of intersection of
c                  gear base circle with involute curve
c
c     values of input variables not changed upon return
c
c-------------------------------------------------
c
c     Notes:
c
c      1.  This method ASSUMES that the center distance cd
c          between the gears is larger than the sum of the c
c          inputs for the base radii rg and rp. There is no
c          error checking !!
c
c      2.  This method assumes that the pinion is the driver
c          rotating clockwise; it is valid for the gear
c          driving counterclockwise.
c
c      3.  This subroutine calls another routine-ANGLE.
c
c      4.  Angle thetag is calculated within the range
c          of {-pi/2 < thetag < 3*pi/2}.
c
c-------------------------------------------------
c
        pi= 4.*atan(1.)
c
c
      call angle(xg,yg,xp,yp,gamma)
c
        gamma = gamma - pi/2.
c
c
        alpha = acos((rp+rg)/
     *       sqrt((xp-xg)*(xp-xg)+(yp-yg)*(yp-yg)))
c
c
        tau = (sqrt((rcpg*rcpg)-(rg*rg))/rg)
c
c
        thetag = pi/2. + alpha - tau + gamma
c
c     restrict the output to -pi/2 < thetag < 3*pi/2
c
        if (thetag .gt. (3.*pi/2.)) thetag=thetag-2.*pi
        if (thetag .lt. (-1.*pi/2.)) thetag=thetag+2.*pi
c
        return
        end

      subroutine pinao(xp,yp,rp,xg,yg,rg,thetag,thetap)
c
c     pinao - FORTRAN subroutine to calculate the PINion
c     Angular Orientation (PINAO)in the global coordinate
c     system. The angular orientation is defined by the
c     angle from the global X-axis to the vector originating
c     at the pinion center and ending at the intersection of
c     the base circle and the involute curve. The returned
c     angle is positive for counterclockwise.
c
c     written by Tim Krantz
c
c     Version  1.0    11/29/93  Original
c     Version  1.1    11/30/93  Revised: Added if statement
c     to restrict variable tau--involute angle of gear--to be
c     less than pi
c
c-------------------------------------------------------
c
c     list of arguments
c
c       inputs
c
c       xp,yp   = global coordinates of pinion center
c       xg,yg   = global coordinates of gear center
c
c       rp      = base radius of pinion
c       rg      = base radius of gear
c
c       thetag  = angular location of intersection of
c                   gear base circle with involute curve
c
c     outputs
c
c       thetap  = angular location of intersection of
c                   pinion base circle with involute curve
c
c     values of input variables not changed upon return
c
c-------------------------------------------------
c
c     Notes:
c
c     1.  This method ASSUMES that the center distance
c         cd between the gears is larger than the sum of
c         the inputs for the base radii rg and rp. There
c         is no error checking !!
c
c     2.  This method assumes that the pinion is the
c         driver rotating clockwise; it is valid for
c         the gear driving counterclockwise.
c
c     3.  This subroutine calls another routine--ANGLE.
c
c     4.  Angle thetap is calculated within the range
c         of {-pi/2 < thetap < 3*pi/2}.
c
c-------------------------------------------------
c
      pi = 4.*atan(1.)
c
c
      call angle(xg,yg,xp,yp,gamma)
```

```
c
      gamma = gamma - pi/2.
c
      alpha = acos((rp+rg)/
               sqrt((xp-xg)*(xp-xg)+(yp-yg)*(yp-yg)))
c
      tau = pi/2. + alpha + gamma - thetag
      if (tau. gt. pi) tau = tau-2.*pi
c
      omega = (((rp+rg) * tan(alpha)) - (tau * rg))/rp
c
      thetap = 3.*pi/2. + alpha - omega + gamma
c
c     restrict output to range -pi/2 < output < 3*pi/2
      if (thetap .gt. (3.*pi/2.)) thetap =   thetap-2.*pi
      if (thetap. lt. (-1.*pi/2.))  thetap = thetap+2.*pi
c
      return
      end


      subroutine angle(x0,y0,x1,y1,zeta)
c
c     angle - FORTRAN subroutine to calculate the angular
c             orientation of a vector.
c     The origin of the vector is at x0,y0.
c     The end of the vector is at x1,y1.
c     The angle is located from the X-axis with angles
c     measured positive counterclockwise.
c
c     written by Tim Krantz
c
c     Version  1.0    11/22/93
c
c-----------------------------------------------------
c
c
c     list of arguments
c
c     inputs
c
c       x0,y0  = global coordinates of vector origin
c       x1,y1  = global coordinates of vector end
c
c     outputs
c
c       zeta   angular location of vector (radians)
c
c-----------------------------------------------------
c
c  Notes:
c
c     1.  The returned angle is in the range (0 <=
c         zeta < 2*pi).
c
c     2.  If the origin and endpoints are identical,
c         the routine will return zeta = pi/2, even
c         though the angle is truly undefined.
c
c-----------------------------------------------------
c
c     Testing
c
c     This subroutine was tested 11/23/93 by Tim Krantz.
c     The correct answer was returned for each of the four
c     quadrants and along each of the four coordinate axes.
c     The subroutine returns zeta = pi/2 if the vector length
c     is zero when actually the angle is undefined.
c
c-----------------------------------------------------
c
      pi=4.*atan(1.)
      dy=y1-y0
      dx=x1-x0
      if (dx) 10,20,10
 10 zeta=atan2(dy,dx)
      if ( zeta .lt. 0.)  zeta=zeta+pi+pi
      return
 20 zeta=pi/2.
      if (dy. lt.0.) zeta=zeta+pi
      return
      end
```

REPORT DOCUMENTATION PAGE

Form Approved
OMB No. 0704-0188

1. AGENCY USE ONLY (*Leave blank*)	2. REPORT DATE	3. REPORT TYPE AND DATES COVERED
	September 1996	Technical Memorandum

4. TITLE AND SUBTITLE
A Method to Analyze and Optimize the Load Sharing of Split Path Transmissions

5. FUNDING NUMBERS
WU–505–62–36
1L162211A47A

6. AUTHOR(S)
Timothy L. Krantz

7. PERFORMING ORGANIZATION NAME(S) AND ADDRESS(ES)
NASA Lewis Research Center
Cleveland, Ohio 44135–3191
and
Vehicle Propulsion Directorate
U.S. Army Research Laboratory
Cleveland, Ohio 44135–3191

8. PERFORMING ORGANIZATION REPORT NUMBER
E–10186

9. SPONSORING/MONITORING AGENCY NAME(S) AND ADDRESS(ES)
National Aeronautics and Space Administration
Washington, D.C. 20546–0001
and
U.S. Army Research Laboratory
Adelphi, Maryland 20783–1145

10. SPONSORING/MONITORING AGENCY REPORT NUMBER
NASA TM–107201
ARL–TR–1066

11. SUPPLEMENTARY NOTES
Prepared for the Seventh International Power Transmission and Gearing Conference sponsored by the American Association of Mechanical Engineers, San Diego, California, October 6–9, 1996. Responsible person, Timothy L. Krantz, organization code 2730, (216) 433–3580.

12a. DISTRIBUTION/AVAILABILITY STATEMENT
Unclassified - Unlimited
Subject Category 37
This publication is available from the NASA Center for AeroSpace Information, (301) 621–0390.

12b. DISTRIBUTION CODE

13. ABSTRACT ***(Maximum 200 words)***

Split-path transmissions are promising alternatives to the common planetary transmissions for rotorcraft. Heretofore, split-path designsproposed for or used in rotorcraft have featured load-sharing devices that add undesirable weight and complexity to the designs. A method was developed to analyze and optimize the load sharing in split-path transmissions without load-sharing devices. The method uses the clocking angle as a design parameter to optimize for equal load sharing. In addition, the clocking angle tolerance necessary to maintain acceptable load sharing can be calculated. The method evaluates the effects of gearshaft twisting and bending, tooth bending, Hertzian deformations within bearings, and movement of bearing supports on load sharing. It was used to study the NASA split-path test gearbox and the U.S. Army's Comanche helicopter main rotor gearbox. Acceptable load sharing was found to be achievable and maintainable by using proven manufacturing processes. The analytical results compare favorably to available experimental data.

14. SUBJECT TERMS
Gears; Transmissions; Helicopters

15. NUMBER OF PAGES
21

16. PRICE CODE
A03

17. SECURITY CLASSIFICATION OF REPORT	18. SECURITY CLASSIFICATION OF THIS PAGE	19. SECURITY CLASSIFICATION OF ABSTRACT	20. LIMITATION OF ABSTRACT
Unclassified	Unclassified	Unclassified	